DR. ARTO MAATTA (Orcid ID : 0000-0003-3759-1310)

Article type : Concise Communications

Pulling force deforms hair follicle root sheath nuclei and surrounding dermal collagen matrix differently at infundibulum, isthmus and suprabulbar regions

Simeon Johnson[1], Kevin Cowley[2], Timothy J. Hawkins[1]*, Arto Määttä[1]*

1) Department of Biosciences, Durham University, Durham, DH1 3LE, United Kingdom.

2) Procter & Gamble, Reading Innovation Centre, Reading RG2 0RX, United Kingdom

*) Corresponding authors: Arto.Maatta@durham.ac.uk and t.j.hawkins@durham.ac.uk

Running title: Hair follicle biomechanics

Abstract

The biomechanical properties of the collagenous dermal matrix are well described but responses to mechanical force by the hair follicles have not been characterised so far. We applied a pulling force on hair follicles to visualise and quantify changes in the keratin-14 and

This article has been accepted for publication and undergone full peer review but has not been through the copyediting, typesetting, pagination and proofreading process, which may lead to differences between this version and the Version of Record. Please cite this article as doi: 10.1111/exd.13948

involucrin positive cell layers of the follicles using nuclear dimensions as an indicator of tissue deformation. Moreover, we used second harmonic generation imaging to visualise changes in the dermal collagen. We report how the anatomical regions of the follicle respond to the force. Nuclei of the isthmus region were most affected. The nuclei in both K14 positive outer root sheath cells and in involucrin positive cells were significantly compressed, whereas the response in the infundibulum and suprabulbar regions was more variable. The deformation of the nuclei did not correlate with lamin A/C expression. The changes in the collagenous matrix were distinct at different depths of the dermis as collagen fibrils were compressed closer to each other in the region adjacent to upper suprabulbar follicle and pulled apart near the infundibulum. Thus, the responses to the force are locally defined and the cells in the permanent and cycling parts of the follicle behave differently.

Keywords: Hair follicle, biomechanics, collagen, Lamin A/C, multiphoton microscopy

Background

Human skin resists mechanical stress by several integrated ways. In the epidermis and hair follicles, cell-cell junctions and cytoskeleton generate the tissue resilience [1, 2]. In the dermis, the extracellular matrix maintains the ability of the skin to resist stretching and compression. The dermis is, furthermore, divided to distinct layers: papillary dermis with loosely arranged collagen fibers, reticular dermis with thick collagen bundles, and hypodermis with collagen bundles among adipose cells. However, the abundant dermal collagen types I and III are found in all dermal layers [3].

Studies on the biomechanical properties of the skin have mostly concentrated on understanding the effects of lateral stretching [4, 5]. Dermal organisation has been investigated using second harmonic generation (SHG), which visualises fibrillar collagens [4, 6-8]. Mechanical response to a force shows behaviour of a viscoelastic material until the dermal tissue ruptures and fails [9]. The response of the collagen fibers can explain the macroscopic effects at the tissue level. Re-organisation of collagens involves alignment of the fibers along the direction of the stretching [4,5, 10].

However, the co-ordination of the responses to mechanical stress in the epidermal and dermal compartments has not been characterised. This is interesting as cell proliferation and differentiation are affected by the biomechanical properties of the underlying matrix [11, 12, 13]. This has implications for hair follicles where the lower part of the follicle undergoes cyclical growth [14] while the follicles are embedded in dermal layers with different matrix densities: infundibulum in the papillary dermis, isthmus in the reticular dermis and the suprabulbar region extending through the reticular dermis into the hypodermis. Intriguingly, several distinct epithelial cell populations are found along the follicle [15]. Characterisation of the mechanical responses at the different anatomical locations can contribute to the understanding of the biology of these cell populations.

Questions addressed

We investigated how the follicle epithelial cells respond to pulling force. To find out where the force deforms epithelial cells, we measured changes in the nuclear shape along the direction of the force. To investigate whether changes in the adjacent dermal collagen matrix correlate with the alterations in nuclear morphology, we visualised collagen fibrils.

Experimental Procedures

To establish a method to study hair follicle biomechanics, we designed a 3D-printed supporting chamber and pulled individual hairs using defined forces (Supplementary Figure 1). Hairs were released from the pull immediately or after a ten minute tension and processed for immunohistochemistry [16]. Collagen organisation was visualised before and after the pull and release by SHG imaging [6-8].

Nuclear dimensions were analysed from longitudinal cryosections at separate regions along anagen follicles [14]. We investigated nuclear morphology in both K14 positive outer root sheath cells [17] and involucrin positive, differentiated cells [18] that also mark the inner root sheath in the suprabulbar region and in the isthmus.

Further experimental details are given in 'Supplementary Materials and Methods'

Results and Conclusions

Differential response to pulling force by hair root sheath regions

We subjected hair follicles (Fig 1A) and the adjacent dermis to a pulling force along the direction of the hair shaft (Supplementary Figure 1). A 2g weight (19.6mN force) resulted in a movement of the hair shaft and surrounding follicle without causing damage or net displacement of the whole skin (Figure 1B and C). Increasing the weight to 5g caused tissue damage or severe deformation of the follicle (Fig 1C). Moreover, the 2g pull and immediate release results in a reproducible movement of the follicle with only a partial immediate return. The median net movement after pull and release was 1.9mm (1.4 to 2.1mm; n=35 follicles).

Keratin-14 cytoskeleton retained its organisation in the infundibulum and isthmus after the mechanical stress resulting from a pull with a 2g weight. In the suprabulbar cells, K14 staining demonstrated some re-alignment along the direction of the applied force (Fig 1D). After a pull and immediate release, the length of the nuclei along the direction of the force did not change in the K14 positive cells in the infundibulum (Fig 1E). On the contrary, there was a statistically significant, 30%, compression in the isthmus while the nuclei of the suprabulbar region were significantly elongated by 16% (Fig 1E). The changes in the nuclear shape were also reflected by an altered nuclear aspect ratio. Pull and immediate release resulted in a lower aspect ratio in the infundibulum and a higher ratio in the suprabulbar area (Supplementary Table 1). After a prolonged pulling before the release, also the nuclei in the infundibulum were compressed and showed a lower aspect ratio while the nuclei in the isthmus had remained compressed (Figure 1D, E, Supplementary Table 1 and Supplementary Figure 2). Thus, the longer application of the force before the release can result in additional changes in the nuclear shape but the main change in the isthmus occurs immediately.

Next, we investigated the response to the force in the involucrin positive cells (Supplementary Figure 3A). In the isthmus, the pull resulted in a lateral widening of the tissue whereas no obvious deformation was seen in the infundibulum (Supplementary Figure 3B). Moreover, the changes in the dimensions of the nuclei in the involucrin positive cells were broadly similar to those seen in the K14 positive cells (Supplementary Figure 3C). In the isthmus, the nuclei were compressed longitudinally (Supplementary Figure 3C and Supplementary Table 2). The change in the isthmus was obvious also after the prolonged pulling of the follicles before the release (Supplementary Figure 3C and Supplementary Figure 4). No statistically significant changes were observed in the inner root sheath nuclei in the suprabulbar regions. In the infundibulum, some decrease of the length of the nuclei was seen in the immediate pull/release experiments ($p < 0.05$). To summarise, the pulling force deforms the nuclei differentially in adjacent

anatomical regions of the follicle. Thus, hair follicles do not respond uniformly to a force. In addition, the extent of the change is not necessarily dependent on the time the force is applied before the release from the pull. The behaviour of the cells in the suprabulbar region may be related to fact that the lower part of the hair follicle extends into the soft hypodermis.

The variation of the nuclear shape changes could depend on how the nuclear envelope withstands stretching. In the nuclear envelope, lamin A/C contributes to resistance against mechanical stress [19]. Lamin A/C immunofluorescence [20] revealed no differences between the anatomical regions of the follicle (Supplementary Figure 5). The expression pattern is in accordance with that seen in the mouse follicles [21]. Thus, our results indicate that lamin A/C expression does not, on its own, define how the nuclei respond to forces.

Collagen matrix adjacent to the follicle is stretched at the suprabulbar region and compressed near the isthmus

Next, we investigated how the pulling force affects the surrounding collagen matrix (Fig 2 A and B). SHG yielded a characteristic fibrillar array distinct from the 2-photon autofluorescence (Fig 2A). *In vitro* collagen gels were used to confirm that SHG detects collagen (Supplementary Figure 6). Trichrome staining confirmed that even in the reticular dermis, where the fiber bundles are generally thicker, the matrix immediately adjacent to the follicle in the dermal sheath comprises thinner collagen bundles (Fig 2B).

The intensity profiles of SHG images show how individual fibril bundles can be distinguished allowing measurement of their spacing (Fig 2C). SHG imaging of the tissue demonstrated how the dermis adjacent to the hair follicle responds to pulling. Near the infundibulum, the

increased average distance between the collagen fibers indicates that the fibrils are pulled apart (Fig 2D). On the contrary, near the isthmus the spacing of collagen fibrils remained unchanged and the fibrils got packed more closely to each other at the suprabulbar region (Figure 2D).

Thus, the dermal matrix responds differently to the force depending on the location along the direction of the hair follicle. Moreover, the changes in the epithelial compartment are not similar to the dermal changes. The overall tissue architecture is likely to affect behavior of collagen fibers. For example, sebaceous glands may contribute to tighter spacing of collagen fibers that are pulled upwards towards the glands from the suprabulbar region. Likewise, the looser arrangement of the ECM in the papillary dermis may facilitate the separation of the fibers near the infundibulum.

Several proteins implicated in protection against mechanical stress are expressed in the hair follicles. Periostin, that is up-regulated by mechanical stress, is expressed in the lower portion of hair follicles [22] and keratinocytes respond to stretching by activation of Akt and p42/44 MAPK signaling [23, 24].

Even though cells of the ORS form a continuous epithelial tissue, we found that the response to the pulling force is not uniform. This is interesting as the different anatomical locations of the follicle harbour functionally distinct cell populations. For example, the region below the isthmus contains cells that are required for maintenance of hair cycling [15, 25]. Our results suggest that it might be interesting to investigate the biomechanical properties of defined cell populations at different hair follicle regions.

Acknowledgements.

We thank Miss Joanne Robson for expert support for microscopy and Mr. Simon Bush for help in designing 3D-printed constructs. The authors have no conflicts of interest to declare. Author contributions: AM, KC and TH planned and directed the project; SJ carried out the experiments; SJ, TH and AM analysed the data, AM wrote the manuscript. This project was funded by a PhD studentship grant from Procter & Gamble.

References

[1] L. Ramms, G. Fabris, R. Windhoffer, N. Schwarz, R. Springer, C. Zhou, J. Lazar, S. Stiefel, N. Hersch, U. Schnakenberg, T. M. Magin, R. E. Leube, R. Merkel, B. Hoffmann, *Proc. Natl. Acad. Sci. USA*, 2013, **110,** 18513-18518.

[2] C. M. Hammer, J. R. Stanley, *Annu. Rev. Pathol.* 2016, **11,** 175-197.

[3] M. El-Domayati, S. Attia, F. Saleh, D. Brown, D. E. Birk, F. Gasparro, H. Ahmad, J. Uitto, *Exp. Dermatol.* 2002, **11,** 398-405.

[4] S. Bancelin, B. Lynch, C. Bonod-Bidaut, G. Ducourthial, S. Psilodimitrakopoulos, P. Dokladal, J-M. Allain, M-C. Schanne-Klein, F. Ruggiero, *Sci. Rep.* 2015, **5,** 17635.

[5] S. Nesbitt, W. Scott, J. Macione, S. Kotha, *Materials*, 2015, **8**, 1841-1857.

[6] P. J. Campagnola, A. C. Millard, M. Terasaki, P. E. Hoppe, C. J. Malone, W. A. Mohler, *Biophys. J*. 2002, **82**, 493-508.

[7] W. R. Zipfel, R. M. Williams, W. W. Webb, *Nat. Biotechnolog.* 2002, **21,** 1369-1377.

[8] I. Gusachenko, Y. Goulam Houssen, V. Tran, J-M. Allain, M-C. Schanne-Klein, *Biophys. J.* 2012, **102,** 2220-2229.

[9] D. L. Bader, P. Bowker, *Biomaterials*, 1983, **4**, 305-308.

[10] B. Lynch, S. Bancelin, C. Bonod-Bidaut, J-B. Guesquin, F. Ruggiero, M-C. Schanne-Klein, J-M. Allain, *Acta Biomater.* 2017, **50,** 302-311.

[11] J. Reichelt, *Eur. J. Cell Biol.* 2007, **86**, 807-816.

[12] J. T. Connelly, J. E. Gautrot, B. Trappmann, D. W. Tan, G. Donati, F. M. Watt, *Nat. Cell Biol.* 210, **12**, 711-718.

[13] B. Trappmann, J. E. Gautrot, J. T. Connelly, D. G. T. Strange, Y. Li, M. L. Oyen, S. M. A. Cohen, H. Boehm, B. Li, V. Vogel, J. P. Spatz, F. M. Watt, W. T. Huck, *Nature Mater.* 2012, **11**, 642.

[14] M. R. Schneider, R. Schmidt-Ullrich, R. Paus, *Curr. Biol.* 2009, **19,** R132-R142.

[15] V. Jaks, M. Kasper, R. Toftgård, *Exp. Cell Res.* 2010, **316,** 1422-1428.

[16] L. M. Sevilla, R. Nachat, K. R. Groot, J. F. Klement, J. Uitto, P. Djian, A. Määttä, F. M. Watt, *J. Cell Biol.* 2007, **179**, 1599.

[17] L. Langbein, J. Schweizer, *Int. Rev. Cytol.* 2005, **243,** 1-78.

[18] M.A. Adly, H. A. Assaf, *Histochem. Cell Biol.* 2012, **138**, 683-692.

[19] J. Swift, I. L., Ivanovska, A. Buxboim, T. Harada, P. C. D. P. Dingal, J. Pinter, J. D. Pajerowski, K. R. Spinler, J-W. Shin, M. Tewari, F. Rehfeldt, D. W. Speicher, D. E. Discher, *Scien*ce, 2013, **341,** 1240104.

[20] J.A. Dyer, I. R. Kill, G. Pugh, R. A. Quinlan, E. B. Lane, C. J. Hutchison, *Chromosome Res*. 1997, **5**, 383-394.

[21] M. Hanif, Y. Rosengardten, H. Sagelius, R. Rozell, M. Eriksson, *PLoS One*, 2009, **4,** e4114.

[22] N. Yoshiba, K. Yoshiba, A. Hosoya, M. Saito, T. Yokoi, T. Okiji, N. Amizuka, H. Ozawa, *Cell Tissue Res*. 2007, **330,** 133-145.

[23] S. Yano, M. Komine, M. Fujimoto, H. Okochi, K. Tamaki, *J. Invest. Dermatol.* 2004, **122,** 783-790.

[24] S. Kippenberger, J. Kleemann, M. Meissner, K. Steinhorst, J. Müller, C. C. Zouboulis, R. Kaufmann, N. Zöller, *J. Dermatol. Sci.* 2018, **89,** 241-247.

[25] J.D. Hoeck, B. Biehs, A. V. Kurtova, N. M. Kljavin, F. de Sousa e Melo, B. Alicke, H. Koeppen, Z. Modrusan, R. Piskol, F. J. de Sauvage, *Nat. Cell Biol*. 2017, **19,** 666-676.

Figure Legends

Figure 1. Histological and multiphoton microscopy approach to analyse hair follicle biomechanics. A) Human hair follicle visualised by keratin-14 staining of the outer root sheath. Brackets show approximate regions within the infundibulum (Inf), isthmus (Isth) and suprabulbar regions (Sup) and representative skin depths where the measurements of the nuclear dimensions were taken. Scale bar =100μm. B) Multiphoton label-free imaging of a hair follicle before the pull and after a pull and release. Dashed lines show the outline of a pulled follicle (hf) and the * signs demonstrate the net movement of the bulb end of the follicle. The panels are stitched together from two separate photomicrographs. Scale bar =500μm. C) Outer root sheath deformation generated by 49.1mN and 19.1mN pulling forces (5g and 2g weights). Dapi staining shows ORS nuclei and the white line defines the location of the basement

membrane. Scale bar =10μm. D) K14 positive ORS cells of the infundibulum, isthmus and suprabulbar regions of control and pulled hair follicles. K14 staining (red channel), DAPI staining (blue) and merged panels are shown. Hair shaft and the dermis adjacent to the follicle are indicated by *H and *D, respectively. Scale bar for all panels is 20μm. E) Nuclear length (mean ± s.e.m. shown) along the direction of the pulling force in K14 positive cells in the infundibulum, isthmus and suprabulbar regions of control follicles, follicles pulled with 2 g weight and immediately released, and follicles pulled and held under tension for 10 minutes before the release. Statistical significance (ANOVA with Tukey's post-hoc test) is shown above the bars: *** $p<0.001$, * $p<0.05$.

Figure 2. Collagen fiber organization in the dermis adjacent to pulled hair follicles. A) Second harmonic generation (SHG) detects collagen fibrils that cannot be distinguished by 2-photon excited autofluorescence (2PEF). B) Masson's Trichrome staining of dermal collagen organisation. Note that the right-hand panel showing the bulb is from the same follicle but different microtome section to the centre and left panels. C) Example of intensity profiles of SHG (red line) and 2PEF (blue line) in the dermis. Collagen fibril spacing can be measured as the distance between intensity peaks. D) Changes in the collagen fiber spacing after pulling force in dermal regions near infundibulum, isthmus and suprabulbar regions. Statistical significance (pairwise T-test) is shown above the bars: * $p<0.05$.

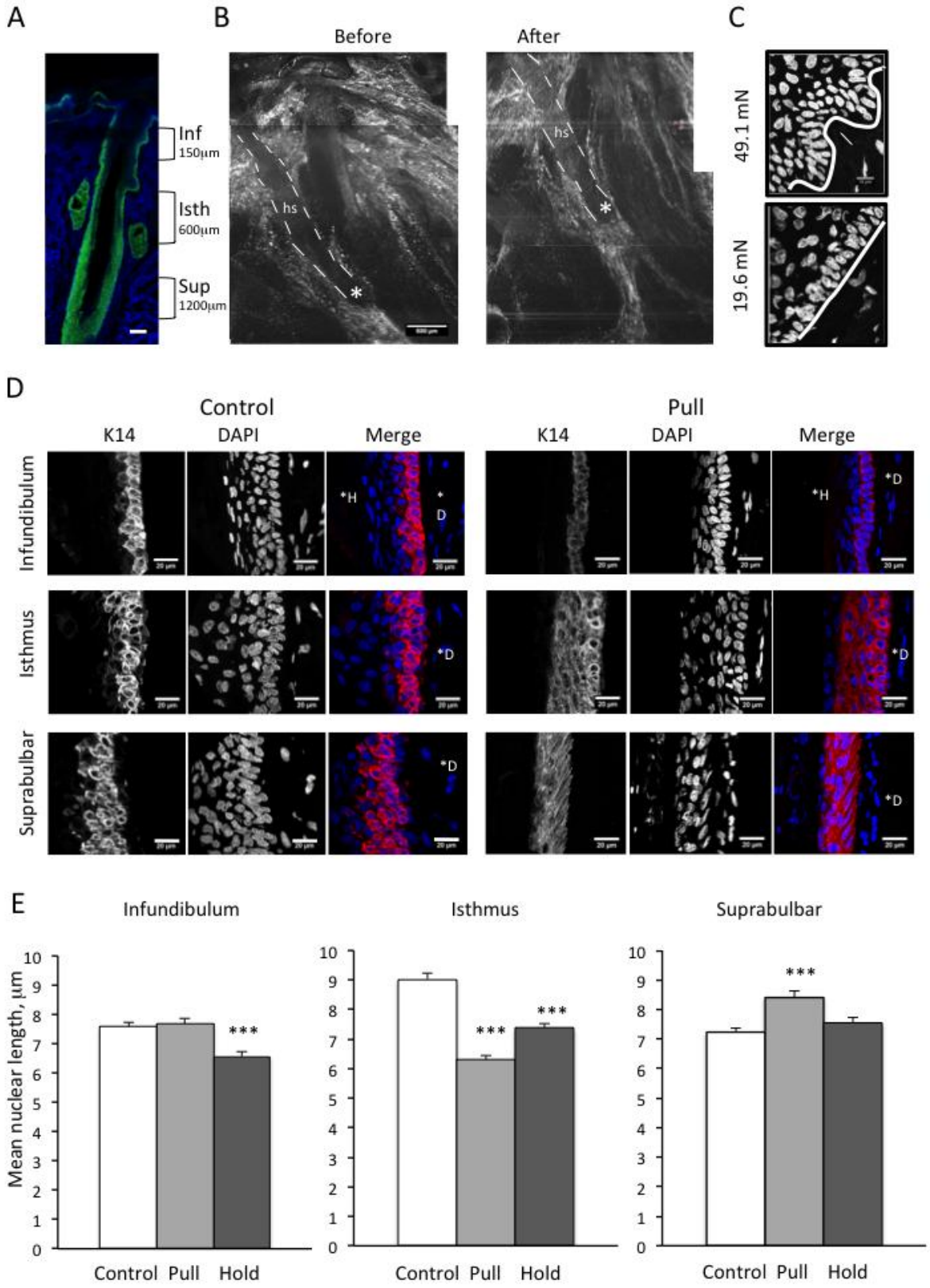

Johnson et al, Figure 1.

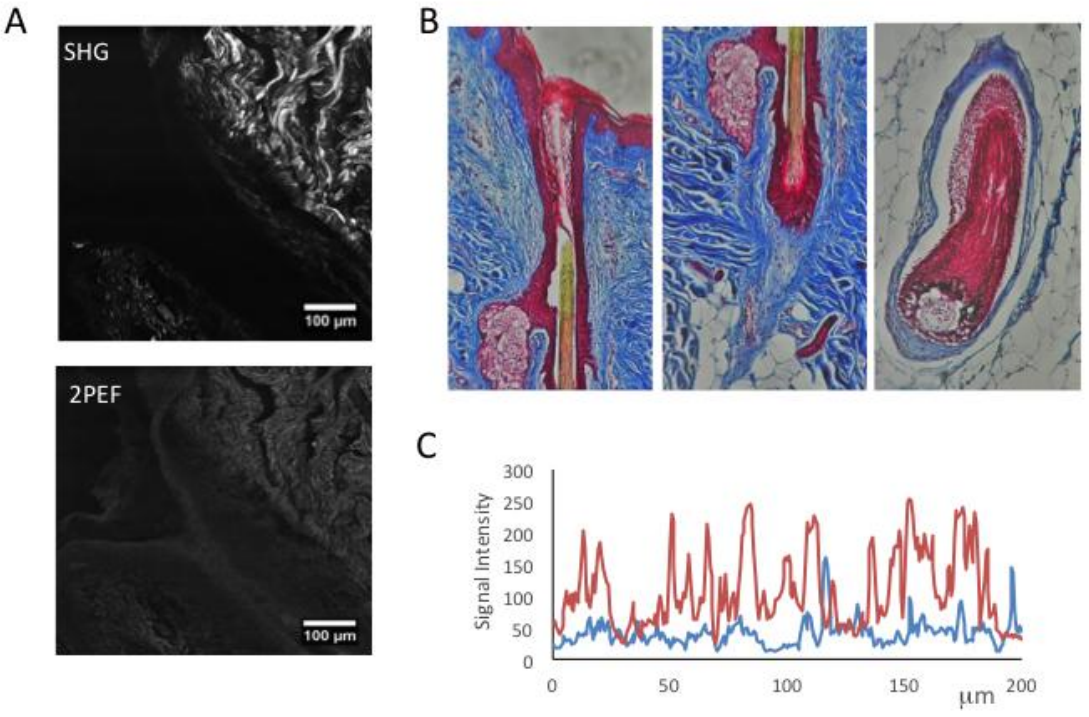

Johnson et al, Figure 2.